

Hand Vein Biometric Verification Prototype: A Testing Performance and Patterns Similarity

Ahmed M. Badawi
Biomedical Engineering Department
University of Tennessee, Knoxville, TN, USA

Abstract - The shape of the subcutaneous vascular tree of back of hand contains information that is capable of authenticating the identity of an individual. In this paper a hand vein verification system was prototyped and statistical performance measures were analyzed. In order to evaluate the system testing performance, a dataset of 500 persons of different ages above 16 and of different gender, each has 10 images per person was acquired at different intervals, 5 images for left hand and 5 images for right hand. Different Biometrics performance measures such as Efficiency, Sensitivity, Specificity, FAR, FRR, EER, and ROC were calculated. Maximum efficiency for the testing set was reported as 99.888 % at threshold equal 78. At this threshold, Sensitivity, Specificity, FAR, FRR were reported as 92.16%, 99.966%, 0.03%, and 7.84%. Finally, we verified that no similarity exists between right and left hand vein patterns for the same person.

Keywords: Biometrics, Verification, Hand Veins, Patterns Similarity, Statistical Performance.

1.0 Introduction

The physical shape of the subcutaneous vascular tree of the back of the hand contains information that is capable of authenticating the identity of an individual [1-4] to a reasonable result which is comparable to our work proposed in this paper. The shape of the finger vein patterns and its use for identification was proposed by [5]. The major goal of our work is to use the combined image processing and pattern recognition knowledge in implementing the Hand Vein Verification System (HVVS) as a comparison between a person's hand vein image and the claimed identity hand vein image based on image matching in order to get a comparable or higher accuracies than those reported in the literature for hand vein verification. The hand vein biometrics principle is a non-invasive, computerized comparison of subcutaneous blood vessel structures (veins) in the back of a hand to verify the identity of individuals for biometric applications. Vein check measures are the shape and size of veins in the back of the hand (or front of the wrist). The vein pattern is best defined when the skin on the back of the hand is taut – when the fist is clenched. The skeleton of the hand then holds the vein “tree” rigid. Non-harmful, near infrared lighting is employed. The vein “tree” pattern is picked up

by CCD video camera with an infrared filter installed on its objective lens to prevent the visible light from reaching its sensor array to construct a pure infrared image for the back of the hand, and converted by a computer into a digital image that can be processed and stored. Figure 1 shows example of hand vein image acquired using our setup. This pattern of the vein “tree” is sufficiently to function as a personal bar code, or PIN equivalent, that is extremely difficult to duplicate or discover. In the 1930s there were a number of publications citing the use of this method in assessing veins in various regions of the body [6]. The infrared region is of special advantage since the skin tissue is relatively transparent and the blood absorbs infrared light well. Hence, the image contrast is higher than in the visible area.

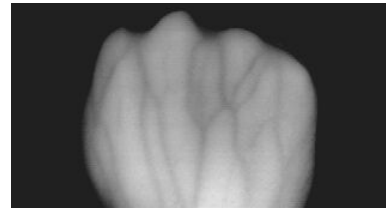


Fig.1. Hand vein image

Since the arrival of fairly low cost CCD cameras and computer power, it seems straightforward to try to consider these technologies [7-8]. Normally, black and white CCD cameras are also sensitive in the near infrared region, so a filter blocking the visible light is all that is needed on the camera. Proper lighting is of course essential to obtain even illumination on the skin surface. The images are transferred to a PC, where some filtering is done. The setup for hemodynamics data acquisition [7-8] is shown in Figure 2. The results are obtained within seconds of the examination. There are many research attempts for the extraction, segmentation and tracing of subcutaneous peripheral venous patterns [9-12], its main aim is to make data reduction and noise suppression for good diagnostic purposes and for making some quantitative measurements like lengths and diameters for the extracted vessel segments. These techniques based on mathematical morphology and curvature (veins direction) evaluation for the detection of vessel patterns in a noisy environment. Researchers in hand vein biometrics [3-5] had a satisfactory result for either verification or identification purposes, regardless of the difference in datasets size, methods, or vein similarities used. The vein tree detection stage includes four consecutive sub stages, which are hand region

segmentation (i.e. region of interest localization and background elimination), smoothing and noise reduction, local thresholding for separating veins, and postprocessing.

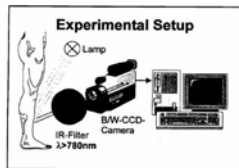


Fig.2. Setup for hemodynamics data acquisition consists of: lighting (halogen), volunteer's leg, IR filter, B/W IR sensitive CCD and IBM compatible PC with a frame grabber for [7-8] group

2.0 Data Acquisition and Processing

In visible light, the vein structure on the back of the hand is not easily discernible. The visibility of the vein structure varies significantly depending on factors such as age, levels of subcutaneous fat, ambient temperature and humidity, physical activity, and hand position. In addition a multitude of other factors including surface features such as moles, warts, scars, pigmentation and hair can also obscure the image. Fortunately, the use of thermographic imaging in the near IR spectrum exhibit marked and improved contrast between the subcutaneous blood vessels and surrounding skin, and eliminates many of the unwanted surface features. The temperature gradient between the veins and surrounding tissue is generally more pronounced than the difference that can be seen by the naked eye. A comparison between visible light image and infrared image for the same person's hand is demonstrated in Figure 3. A commercially available conventional charge-couple device (CCD) monochrome camera, rather than a considerably more expensive thermal camera, is used to obtain the thermal image of the back of the hand [13]. Though principally designed for use in visible light, CCD cameras are also sensitive to near IR wavelengths of the electromagnetic spectrum up to about 1100 nm. This is an actinic IR range, which covers the near infrared spectrum from 700 nm to 1400 nm.

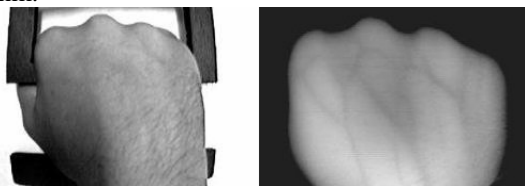


Fig.3. Visible light image (left) and IR image (right) for the same person

We have chosen a camera that is highly sensitive in the near infrared region (see the camera characteristic curve in Figure 4). The greatest intensity of IR radiation emitted by the human body is 10 mW/cm² in the range of 3000-14000 nm [1]. Unfortunately the CCD camera has no sensitivity in this region. Furthermore any naturally emitted near IR radiation is far too weak to be detected by the camera's CCD imager. Consequently after experimentation with a variety of light sources, including high intensity tungsten lamps, it was found to be necessary to irradiate the back of

the hand using an IR cold (solid-state) source. The reduced hemoglobin in venous blood absorbs more of the incident IR radiation than the surrounding tissue thus appearing darker when viewed on a conventional PC monitor.

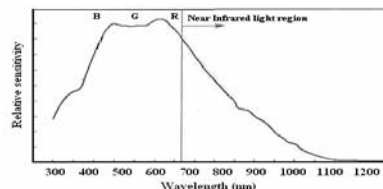


Fig.4. Spectral sensitivity characteristics of used silicon based CCD sensor

The depth of absorption and radiation of actinic IR in biological tissue is approximately 3 mm, and so thermal IR radiation provides information only about surface (skin) temperatures of biological objects [1]. As a consequence only the subcutaneous vascular network is discernible in the image. The quality and extent of the revealed vein structure is however highly variable. In our prototype we have designed a near IR cold source to provide back-of-hand illumination. The IR cold source is a solid-state array of 24 LEDs (light emitting diodes). The diodes are mounted in a square shape, 6 LEDs in each side, on a designed and assembled PCB (printed circuit board). We made a housing and an attachment for fixing the LEDs around the CCD lens. Our experiments showed that the cold source provides better contrast than the ordinary tungsten filament bulbs. A commercially available, low cost, monochrome CCD fitted with an IR filter is used to image the back of hand. The transmission curve for the used filter (Hoya RM90) is shown in Figure 5. The curve reveals that the filter has a small tail of transmittance down to about 750 nm. The IR filter ensures that no visible light reaches the CCD sensor. After using the cold IR light source and the IR filter, the image constructed on the CCD sensor is totally a thermal graph for the back of the hand. When seen on the computer monitor, the mostly distinguishable component in the image is the superficial vein tree pattern. A simplified schematic diagram for our hand vein image acquisition prototype module is demonstrated in Figure 6. We have designed a hand attachment frame for constraining the person's hand; it is suitable for the right and left hand as shown in Figure 7. The hand is presented as a clenched fist with the thumb and all the other fingers are hidden. It allows a person to easily position his/her hand in front of the camera and it eases the shape matching search process (translation and rotation variations). The attachment frame is painted with poster black, flat acrylic, scenic paint to minimize reflection of IR radiation from their surfaces.

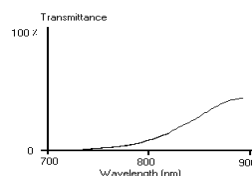


Fig.5. Transmission curve for the RM90 IR filter

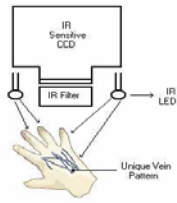


Fig.6. Schematic of the hand vein imaging module

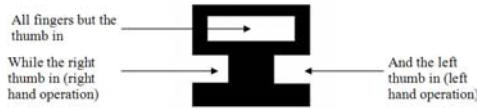


Fig.7. Hand attachment frame

The intensity of IR source is attenuated by the use of diffusing paper and it helps for obtaining an equally distributed illumination on the hand area. A monochrome frame-grabber is used to capture an image of the back of a hand for computer processing. Images are captured using a 320W X 240H pixels video digitizer with a gray-scale resolution of 8-bits per pixel. A sample hand vein image from our data set is shown in Figure 8 for a male hand.

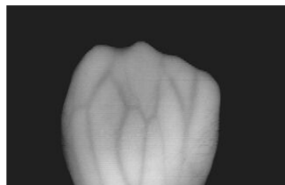


Fig.8. Acquired image of 320W X 240H pixels, 8-bits per pixel

2.1 Hand Vein Image Processing Stages

This is the second stage in the Hand Vein Verification System (HVVS), which covers the detection of vein structures from the acquired infrared image for the back of the hand. The vein tree detection stage includes four steps, which are hand region segmentation (i.e. region of interest localization and background elimination), smoothing and noise reduction, local thresholding for separating veins and finally the postprocessing. Figure 9 illustrates the block diagram of the processing stage.

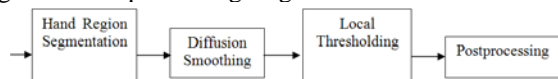


Fig.9. Block diagram of processing stage

2.2 Hand Region Segmentation

Image segmentation is one of the most important steps leading to the analysis of processed image data. Its main goal is to divide an image into parts that have a strong correlation with objects or areas of the real world contained in the image. Binarization is the case of segmenting the image into two levels; object (hand region) and background; the object segment which is the region of interest (ROI) in white and the background segment in black as shown in Figure 10. The algorithm used in the

segmentation sub stage is an iterative method used for calculating and selecting an optimal threshold, which is used to segment the image into two distinct parts; hand and background [14]. We used this resultant binary image to calculate the center of gravity (COG) for our ROI (hand region). Then we translated the grayscale hand region to the center of the image after assigning the background area to zero value pixels. Thus we completely localized, separated and centered the hand region for subsequent processing steps as shown in Figure 10.



Fig.10. Segmentation results; (a) Input gray scale image (b) Binary image and (c) Output image after ROI determination and centering

2.3 Smoothing and Noise Reduction

Two approaches could be used for noise filtering. One approach is using Gaussian blur filter. The disadvantage of Gaussian filter that it is not an edge preserving technique, since it blurs the image with equal weights, which also blurs edges of the veins after several iterations. The second approach is an edge-preserving technique like nonlinear diffusion [17-18]. Perona-Malik is used in which use only image gradient to weight the diffusion process. Figure 11 shows the block diagram of the smoothing filters used in this work where we used a median filter of 5*5 mask in order to remove the hand traces from the acquired image then we used the nonlinear diffusion filter based on edge weighted diffusion in order to smoothen the image while preserving the vein edges. The smoothing and noise cleaning sub stage effect is shown in Figure 12 for 5 iterations of nonlinear diffusion, while the edges are not affected.



Fig.11. Block diagram of smoothing and noise reduction stage

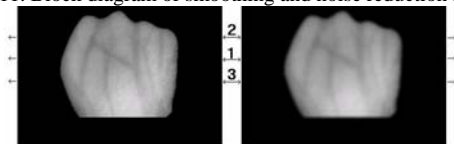


Fig.12. Effect of smoothing sub stage on the image line profiles

2.4 Hand Vein Pattern Segmentation

Specifically, hand vein segmentation is to divide a hand vein image into a foreground (veins in the back of the hand) and a background (non-vessel areas). Segmentation methods can be divided into four groups, which are

threshold-based segmentation, edge based segmentation, region based segmentation and segmentation by matching. In this study, the first thresholding method is adopted since it is computationally cheap and fast. Considering that we want to process and study veins only, global thresholding (i.e. single threshold for the whole image) is not a good technique for this purpose. A better approach is to calculate the average around each pixel of the image in an area of $N \times N$ neighbor pixels and to use average value as a threshold value [12]. The local threshold process separates the vein pattern from the background; hence the desired vein image is extracted. Experimentally we have chosen a 31×31 mask size for computing the threshold for binarizing the central pixel. The result is shown in Figure 13.

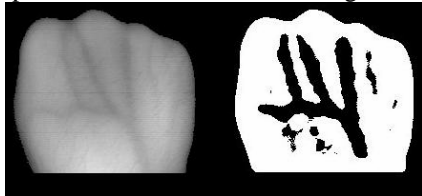


Fig.13. Processed image (left) and its local thresholded image (right)

2.5 Hand Vein Pattern Postprocessing

It is demonstrated from Figure 13 that the resultant binary hand vein contains some noise and un-sharp edges. We experimentally applied 5×5 median filter for improving and validating the output binary hand vein pattern and for reducing the effect of these unwanted defects [14]. We also converted the vein pattern into white in a black background which in this case the entire image. The final pattern after the post processing sub stage is shown in Figure 14.

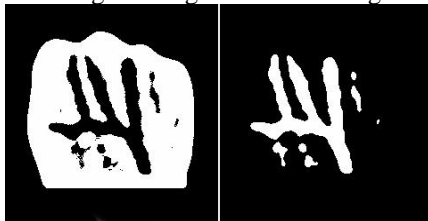


Fig.14. Hand vein pattern before (left) and after postprocessing (right)

2.6 Matching of Hand Vein Patterns

After image acquisition and hand vein extraction sub stages, we have a binary image contains the segmented back of the hand vein pattern. This is suitable for the next and the final sub stage, the matching of hand vein patterns. As it is expected, the input for the matching sub stage is two binary hand vein binary images like the one in Figure 14 (right), the matching output is Yes (the two images are for the same pattern) or No (the input images is not correlated). We used rigid registration technique [15] since we already constrained our data acquisition system with the attachment in order to prevent any large translation or rotation. One of the two images is remained stationary while we apply 2D transformation (x-translation, y-

translation and rotation) on the other image in order to align it with the first pattern (Registration) to find the maximum correlation percentage between two hand vein images. However Fujitsu researchers have presented a contactless/touchless palm vein authentication which is more convenient and non hygienic for users we restricted our designed prototype for a contact system type in order to simplify our matching phase and derive a dependent statistical measures for this proposed prototype. However accounting for scale (Age or hand to camera distance) in the registration algorithm is simple, we did not account for the scale in our matching. In real systems capturing the hand template at equal monthly intervals after correct authentication is suggested in order to track the changes in the hand with age. The matching (similarity) percentage is calculated as the ratio of the count of overlapped white pixels between input images to the number of white pixels in one of the two input images (the image with the minimum count of the white pixels). We calculated the matching ratio for each transformation step then we choose the maximum ratio as the final matching ratio between the two input hand vein patterns. In our implementation and for saving time of matching, we made the parameters (x-translation, y-translation and, rotation) steps equals five, getting the maximum matching ratio on this grid, finally we made a fine search (tune) to find the overall maximum correlation ratio. The result of matching sub-stage is shown in Figure 15, in case of correct true match it is demonstrated that the resultant pattern is correlated to the input images and it is shown that the matching ratio is 81.87 % (same person). A case of correct mismatch is shown in Figure 16, it is shown that the matching ratio is small as 48.27 % (different persons).

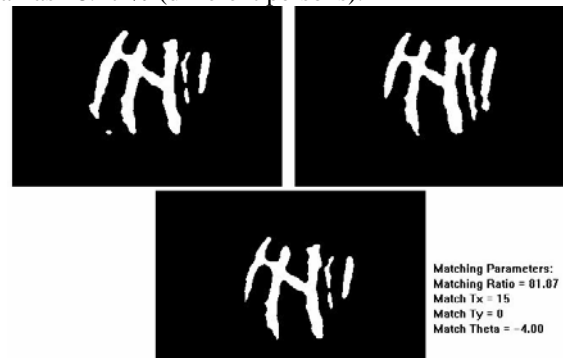


Fig.15. Example of true match for different patterns of the same person



Fig.16. Example of correct mismatch between different persons

3.0 Statistical Performance Measures

3.1 Statistical Results

The system was tested over a database collected using the designed system consisting of 500 persons of different age and gender for each 5 left and 5 right images were acquired. The person was asked to put his/her right hand on the hand attachment frame and the system operator captures the first image for the current person right hand veins. Then the person replaces his/her right hand with the left one for acquiring the first image for the left hand vein pattern. This process was repeated until we acquire five images for the right hand and five images for the left hand in different scenes (5 minutes interval between every acquired image) independent of each other, i.e. ten images for each person. We will prove in our statistical analysis that the hand vein pattern is unique to some level for each person and for each hand. Thus we considered as if we have 1000 persons of which 5 images are in the dataset since we found that left and right hand vein images are different. In order to find the dissimilarity threshold in correlation ratio between the 1000 subjects we have chosen only the first image pattern for each of the 1000 subjects and for a correlation ratio threshold that exceed 80%, we achieved 100% classification (Distinct pattern). For evaluating (testing) our system for verification purpose, all possible comparisons are made between the whole data. We matched each image from our data set with all the 5000 hand vein images in our data set and then we recorded the matching ratios. We constructed the correlation matrix for representing the matching result between each image and all other images. The schematic of our correlation matrix is shown in Figure 17 (Example for 5000*5000); it is filled with the matching ratios between the image in the row label and the image in the column label. The black areas inside the matrix frame in Figure 17 are the areas that the genuine accepts are expected (Ones for same person images after thresholding) while the white ones where the genuine rejects are expected (zeros for different person images after thresholding). We shall use the thresholded correlation matrix for calculating the efficiency of our system at each threshold. Also, we deduced that the optimal threshold at which the maximum efficiency occurs in our system. We performed statistical analysis for selecting an optimal threshold to get the highest system performance, by testing the system over the whole database - exhausting the whole database. To evaluate the hand vein performance we used measures of performance, which include: sensitivity, specificity, false accept rate (FAR), false reject rate (FRR), and efficiency. Figure 18 and Figure 19 shows graphically how GAR(%), and GRR(%) change with different thresholds. Figure 20 and Figure 21 shows graphically how FAR(%), and FRR (%) change with different thresholds. Our aim is to select an optimal threshold. We want a single criterion, such that it takes into account the maximization of true events (GAR, GRR) and minimization of error events (FAR, FRR).

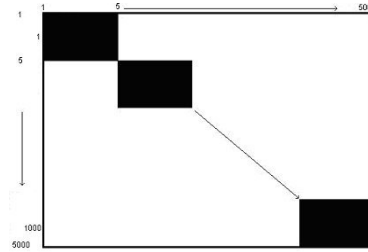


Fig.17. Correlation matrix schematic

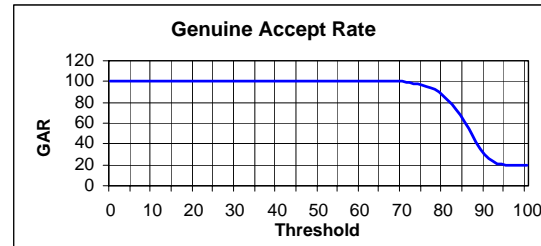


Fig.18. Genuine Accept Rate (GAR) at different thresholds

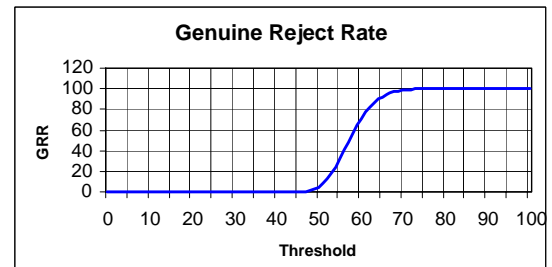


Fig.19. Genuine Reject Rate (GRR) at different thresholds

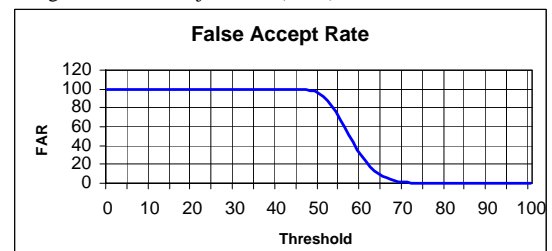


Fig.20. False Accept Rate (FAR) at different thresholds

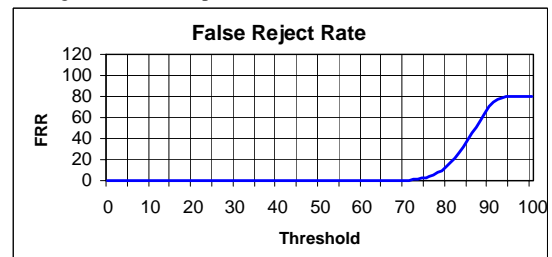


Fig.21. False Reject Rate (FRR) at different thresholds

Figure 22 illustrates the change of system performance at different thresholds. Efficiency, which we will consider as our criterion for evaluating the system performance at different thresholds, reaches its maximum of about 99.888% at a threshold of 78. At this threshold the Sensitivity is 92.16%, the Specificity is 99.966%, FAR is 0.03%, and FRR is 7.84%. Another important curve is the Receiver Operating Characteristic (ROC) curve, which is shown in Figure 23. A receiver operating curve provides an empirical assessment of the system performance at different

operating points which is more informative than FAR and FRR.

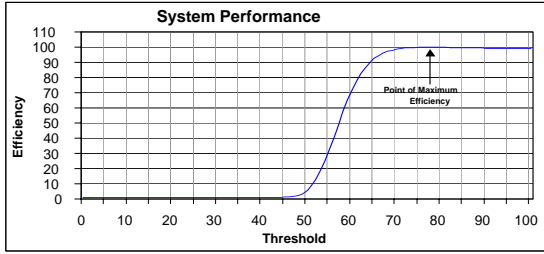


Fig.22. System Performance (Efficiency) at different thresholds

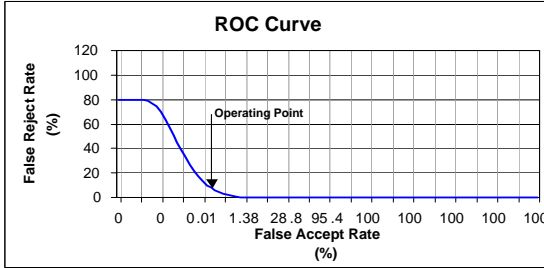


Fig.23. ROC curve for the hand vein verification system (Non-uniform Log Scale)

Hand Vein Verification System (HVVS) is accurate in the low to median security level: e.g., for a threshold 75 the genuine acceptance rate is 96.72% for only a 0.18% false acceptance rate. Although the 0.18% false acceptance rate may seem high, in practice it is much smaller, since a user of the system does not know the identity of which other user he can claim such that their hand veins match. Figure 24 demonstrates FAR(%) and FRR(%) curves on the same graph. To get around this, vendors often provide a variable threshold setting, which allows the customer to strike a balance. If a site needs near 100 percent rejection of impostors, authorized users will have to pay for it in some percent rejection rate. A commonly used point to examine the quality of performance is to evaluate Equal Error Rate (EER) point and it assumes that the costs of FA and FR are equal, and that the class prior probabilities (of client and impostor distributions) are also equal. From Figure 24 we get an ERR for the test data = 0.695% at Threshold = 72.

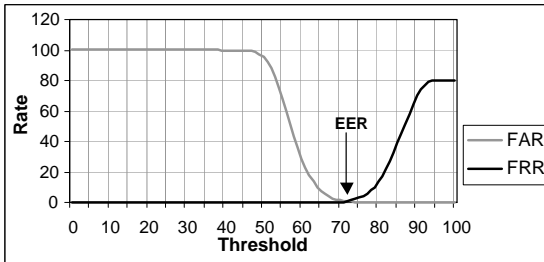


Fig.24. FRR (Type I Error) versus FAR (Type II Error)

3.2 Similarity between Right and Left Patterns

A previous study on the individuality of fingerprint was done in [19] in order to prove the uniqueness of fingerprint features. In the previous section we proved that the hand

vein pattern is unique to some extent for each identity (person), in this section we will estimate the probability for the true match between the right and left hand vein patterns for the same identity. If this probability is low, we will decide that the hand vein patterns are unique for each identity and are unique for each hand i.e. the hand vein pattern for the right hand is different from the hand vein pattern for the left hand for the same person. Else if the resultant estimated probability value is large, we will conclude that the hand vein patterns are unique for each identity but not unique for each hand. Using the correlation matrix, we calculated the mean and standard deviation for the matching ratios between the right and left hand vein pattern for the same person [16]. We calculated the probability for the matching ratio to be greater than the threshold we determined in the previous section. The probability of the matching ratio to be greater than 78% (for deciding a true match), is the probability for the two hands (right and left) for the same person to have a similar vein pattern. Table 1 shows the probability values for the thresholds range from 72% to 80%.

Table 1: Statistical results for the performance of the system, Probability for the true match between the right and left hand vein patterns for the same identity

Threshold (%)	Mean	STD. DEV.	Z = (Thres. - Mean) / Std.Dev.	P(Z)	0.5-P(Z)	P(Similarity >= Threshold) %
72	58.106972	5.53356841	2.51068153	0.494	0.0060	0.60
73	58.106972	5.53356841	2.691396744	0.4964	0.0036	0.36
74	58.106972	5.53356841	2.872111958	0.4979	0.0021	0.21
75	58.106972	5.53356841	3.052827172	0.4989	0.0011	0.11
76	58.106972	5.53356841	3.233542386	0.4994	0.0006	0.06
77	58.106972	5.53356841	3.414257623	0.4997	0.0003	0.03
78	58.106972	5.53356841	3.594972815	0.4998	0.0002	0.02
79	58.106972	5.53356841	3.775688029	0.4999	1E-04	0.01
80	58.106972	5.53356841	3.956403243	0.5	0	0

The probability at the threshold that gave us the maximum efficiency in the previous section (78%) is Probability (Similarity >= 78%) = 0.0002. The calculated probability is small enough to some extent in order to let us conclude that the hand vein patterns are unique for each identity and is unique for each hand i.e. the hand vein pattern for the right hand is different from the hand vein pattern for the left hand for the same person to that shown extent. Figure 25 shows two hand vein images for the same person, the left one for his left hand and the right one for his right hand.

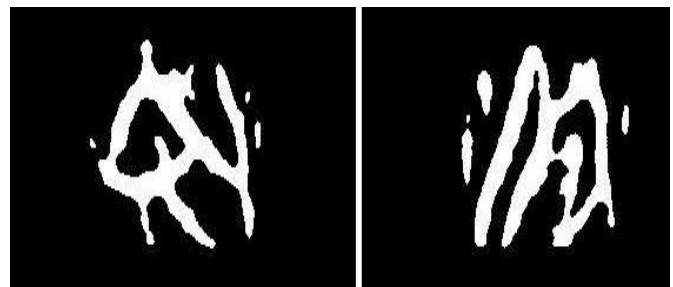


Fig.25. Two-hand vein patterns for the same person, left and right hand

4.0 Conclusions

The designed system was tested for verification purpose only over a database collected with the designed system. Dataset for 500 persons of different age and gender of which ten images per person were acquired (five for the right hand and five for the left) in different scenes at different intervals and are independent of each other, i.e. ten images for each person. Verification performance statistical parameters were estimated for the overall system such as: Genuine Accept Rate (Sensitivity), Genuine Reject Rate (Specificity), False Accept Rate (FAR), False Reject Rate (FRR), Efficiency and Receiver Operating Curve (ROC). System testing performance (overall efficiency) was found to be 99.88% at threshold (matching ratio) equal 78. At this maximum efficiency the Sensitivity is 92.16%, the Specificity is 99.966%, FAR is 0.03%, and FRR is 7.84%. However the difference in methods, datasets, and algorithms that were found in the hand biometric work of [1-5, 22], our performance results are comparable. Finally, we studied the similarity between right and left hand vein pattern for the same person. We verified that the hand vein pattern is unique for each person and is also unique for each hand.

Acknowledgement

Dr. Mohamed S. Kamel and Eng. Mohamed Khairy at Cairo University are acknowledged for their assistance in prototype preparation and their helpful comments.

5.0 References

[1] J. M. Cross and C. L. Smith, "Thermographic imaging of the subcutaneous vascular network of the back of the hand for biometric identification", Proceedings of 29th International Carnahan Conference on Security Technology, Institute of Electrical and Electronics Engineers, 20-35, 1995.

[2] Sang-Kyun Im, Hyung-Man Park, Young-Woo Kim, Sang-Chan Han, Soo-Won Kim, Chul-Hee Kang and Chang-Kyung Chung, "An Biometric identification system by extracting hand vein patterns", Journal of the Korean Physical Society, 38(3): 268-272, March 2001.

[3] Toshiyuki Tanaka, Naohiko Kubo, "Biometric authentication by hand vein patterns" SICE, Annual Conference in Sapporo, 249-253, Aug. 2004.

[4] C.L Lin, K.C. Fan, "Biometric verification using thermal images of palm-dorsa vein patterns", IEEE Trans Circuits Sys Video Tech, 14(2): 199-213, Feb. 2004.

[5] N. Miura et al., "Feature extraction of finger-vein patterns based on repeated line tracking and its application to personal identification", Machine Vision and Applications, 25: 194-203, 2004.

[6] H. Haxthausen, "Infrared photography of subcutaneous veins", Br. Journal. Dermatol., 45, 1933.

[7] Olaf Such, "Near Infrared imaging of hemodynamics",

Proceedings of 18th International Conference of the IEEE/EMBS, Amsterdam, Nov. 1996.

[8] Olaf Such, Sabine Acker and Valdimir Blazek, "Mapped hemodynamic data acquisition by near Infrared CCD imaging", Proceedings of 19th International Conference of the IEEE/EMBS, Chicago, Oct. 1997.

[9] Eric K. Y. Chan and John A. Pearce, "A Rule-Based, adaptive window-size filter for the enhancement of subcutaneous vascular patterns in thermographic images", Proceedings of 11th International Conference of the IEEE/EMBS, 1746-1748, Oct. 1989.

[10] Eric K. Y. Chan and John A. Pearce, "Visualization of dynamic subcutaneous vasomotor response by computer-assisted thermography", IEEE Transactions on Biomedical Engineering, 37(8): 786-795, August 1990.

[11] Eric K. Y. Chan and John A. Pearce, "A Computer-assisted thermography system for the extraction, visualization and tracing of subcutaneous peripheral venous patterns", IEEE International Symposium on Circuits and Systems, 1: 508-511, 1991.

[12] Y. Sun, "Automatic identification of vessel contours in coronary arteries in arteriograms by an adaptive tracing algorithm", IEEE Transactions on Medical Imaging, 8(1): 78-88, March 1989.

[13] F. Van Der Heijden, "Image Based Measurement Systems", John Wiley & Sons, 1995.

[14] Milan Sonka, Vaclav Hlavac and Roger Boyle "Image Processing, Analysis and Machine Vision", Chapman & Hall, 1993.

[15] Robert J. Schalkoff, "Pattern Recognition: Statistical, Structural and Neural Approaches", John Wiley & Sons, 1992.

[16] A. Papoulis, "Probability, Random Variables and Stochastic Processes", Third Edition, McGraw-Hill, New York, 1991.

[17] K.Z. A., Youssef, A. M., and Kadah, Y. M. "Real-Time speckle reduction and coherence enhancement in ultrasound imaging via nonlinear anisotropic diffusion", IEEE Transactions on Biomedical Engineering, 49(9): 997-1014, 2002.

[18] Rushdi, M. A. "Speckle Reduction in Medical Ultrasound Images Using Weighted Diffusion, Neural Networks, and Fuzzy Logic", Master Thesis, Cairo University, 2005.

[19] S. Pankanti, S. Prabhakar, and A. Jain, "On the individuality of finger prints", IEEE Trans on Pattern Analysis and Machine Intelligence, 24(8): 1010-1025, Aug. 2002.

[20] A. K. Jain, S. Prabhakar, L. Hong, and S. Pankanti, "Filterbank-based fingerprint matching", IEEE Trans on Image Processing, 9(5): 846-859, 2000.

[21] A. K. Jain, L. Hong, and R. Bolle, "On-line fingerprint verification", IEEE PAMI, 19(4): 302-314, 1997.

[22] R. Sanchez-Reillo, C. Sanchez-Avilla, and A. Gonzalez-Macros, "Biometrics identification through hand geometry measurements", IEEE Tans PAMI, 22(18): 1168-1171, 2000.